In Situ Observations of Cirrus Clouds from the 1994 ARM RCS IOP

M. R. Poellot and K. A. Hilburn
University of North Dakota
Grand Forks, North Dakota

W. P. Arnott
Desert Research Institute
Reno, Nevada

K. Sassen
University of Utah
Salt Lake City, Utah

Introduction

The Atmospheric Radiation Measurement (ARM) Program Remote Sensing Intensive Observation Period (IOP) was conducted at the Southern Great Plains (SGP) site in April 1994. The University of North Dakota (UND) Citation aircraft was flown during this IOP to gather in situ measurements of microphysical, aerosol, and state parameters of the atmosphere for comparison with ground-based remote sensing observations. Microphysical data collected in cirrus clouds are being analyzed to better understand the particle size distributions, ice water contents (IWCs), and crystal habits of these clouds. These parameters are important to the proper modeling and monitoring of cirrus and their radiative effects. Data from five flights in cirrus are being presented to show how the cloud microphysics varied with cloud forcing, temperature, and position in cloud. Comparisons are also made with observations from the FIRE (First International Satellite Cloud Climatology Program [ISCCP] Regional Experiment) Cirrus Intensive Field Observation (IFO) - II project.

Methodology

The cloud microphysical observations used in this analysis were obtained with a particle measuring system (PMS) two-dimensional cloud (2DC) optical array probe and a formvar replicator supplied by the Desert Research Institute (DRI). In general, replicator images can be analyzed to provide size and number concentration for cirrus particles as small as 10 μm in diameter and they also give detailed information about crystal habit. However, due to the breakup of particles larger than 200 μm or so, the two-dimensional (2-D) probe data provide a better characterization of the larger cirrus particles. In addition, the 2-D data are in digital form, which lends itself to rapid automated processing; analysis of the replicator images is slow and labor-intensive.

This study used a combination of replicator data for particles smaller than 150 µm and 2DC data for the larger ones to produce average particle size distributions. The replicator analysis was performed by DRI and yielded distributions of particle size, area and mass, and also the distribution of particle habits. Unfortunately, it has been determined that the probe was probably undersampling particles smaller than approximately 50 µm, so the particle spectra have been limited by this lower threshold. The 2DC data have been processed to derive particle size spectra and ice water contents for the larger cloud particles.

There were a total of five flights in cirrus during the IOP when data are available for both instruments: April 15, 21, 24, 25, and 29. It has been determined through analysis of satellite and synoptic data that three of these flights (the 24th, 25th and 29th) took place in cirrus generated by thunderstorms, while the other cirrus clouds were formed through lifting associated with shortwave troughs. The analyses are thus presented in terms of convective ("anvil") and non-convective ("non-anvil") cirrus. Flight segments were chosen to represent the various temperature regimes of each mission, and 10-second intervals of replicator data were analyzed for each segment. A total of 33 samples with good replica were analyzed. The University of Utah analyzed their Polarization Diversity Lidar (PDL) data with an algorithm to identify cloud top and base, superimposing the Citation time-height profile on the cloud images (as in Figure 1). They also provided images from the Pennsylvania State University 94-GHz cloud radar for several of the flights. It appears that both remote sensing systems were attenuated at times by the dense anvil sampled on April 25.
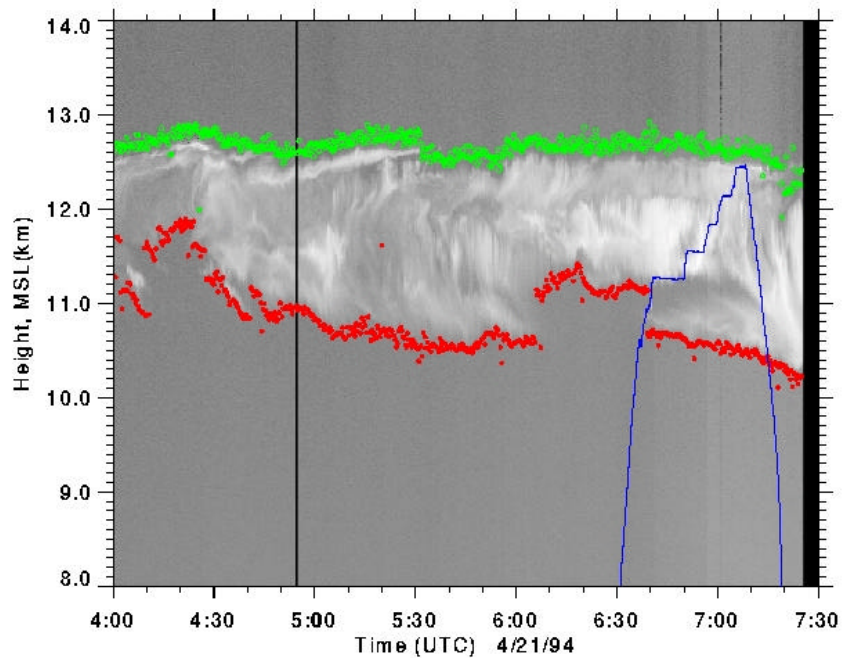

Figure 1. University of Utah lidar time-height cross section for April 21, 1994. The blue line represents plot of altitude vs. time for UND Citation aircraft.

Results

Particle Size Distributions

For the purpose of comparison with previous cirrus studies, some of the average size distributions have been fit with a power law function of the form

$$N = A \, D^B.$$

The shape of the curves can be fairly well approximated through the use of two sets of coefficients, one for the smaller sizes and one for the larger. Both the convective and the non-convective ARM samples have been compared with non-convective cirrus studied during the FIRE cirrus study (Poellot et al. 1998), and frontal overrunning cirrus studied by Heymsfield and Platt (HP, 1984). The size spectra were averaged over 5 °C temperature intervals.

Average spectra for the ARM cirrus as a function of temperature are shown in Figure 2; plots of the power law best fit curves are shown in Figure 3. Table 1 contains values for average IWC, number concentrations for particles with diameters of 100 μm and 1000 μm (N_{100}, N_{1000}), and the slope coefficients for the small (B1) and large (B2) portions of the curves. Both the anvil and non-anvil clouds showed trends of having more large particles and fewer small particles at warmer temperatures. The points of inflection in the fitted curves occur at the intersection of the best fit for smaller and larger particles which is approximately at a secondary mode in the average particle spectra. This mode is seen to move toward small particles at colder temperatures. When the anvil and non-anvil distributions are compared, there are many more large (>200 μm) particles in the anvil than in the non-anvil clouds at both warm and cold temperatures. Numbers of smaller particles, however, are more similar in warm clouds.

Figure 4 presents a comparison of cirrus from ARM, FIRE, and HP. At cold temperatures, the anvil clouds contained more particles than the others at all sizes. The shapes of the anvil and FIRE distributions were similar, while the ARM non-anvil curve had a steeper slope at the small sizes. The HP curve showed no bi-modal tendencies, with the lowest concentrations of medium-to-small size particles. At warm temperatures, the anvil clouds again had the most large particles, but had fewer small particles than either the FIRE or HP clouds. The anvils matched number concentration, curve shape and inflection point more closely with the ARM non-anvil cirrus.

To show the variability of the sampled distributions, the size spectra for the three anvils, the ARM non-anvil and the FIRE clouds are presented for two temperatures in Figures 5 and 6. In both the warm and cold cloud samples, the number concentrations of small particles (~≤ 125 μm) were similar with the exception of the April 29 anvil. Greater differences between the anvils can be seen for sizes larger than about 500 μm.
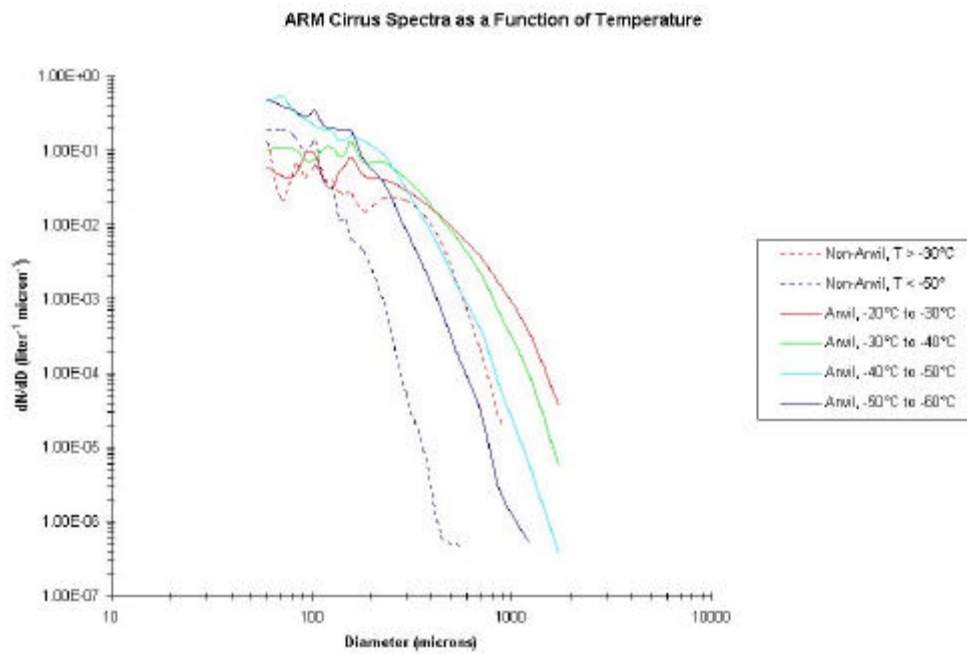
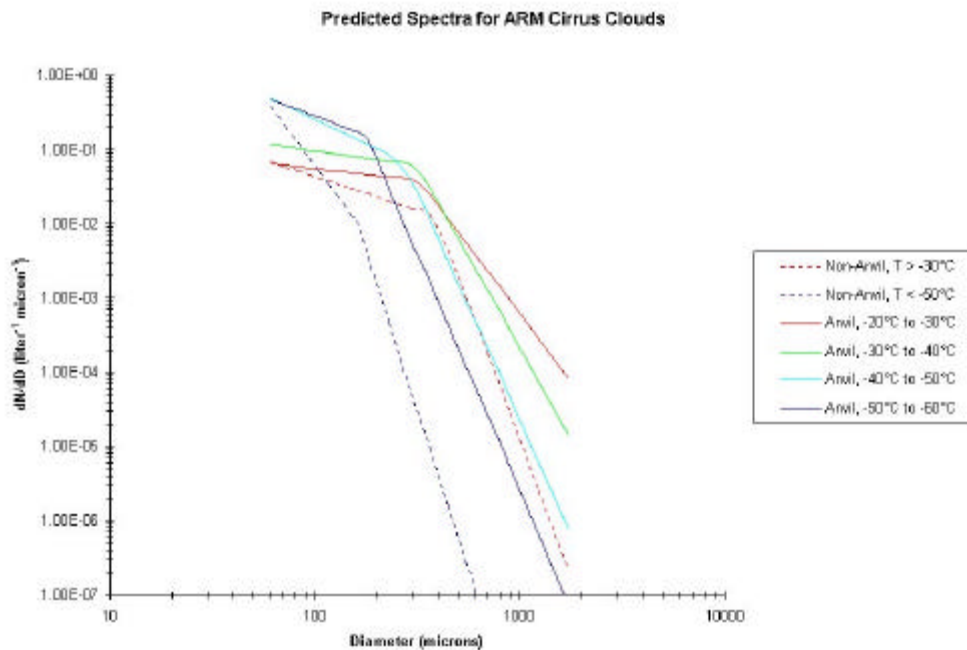**Figure 2**. ARM cirrus particle size spectra as a function of temperature.

Figure 3. Best-fit power law curves for ARM cirrus cloud size distributions.

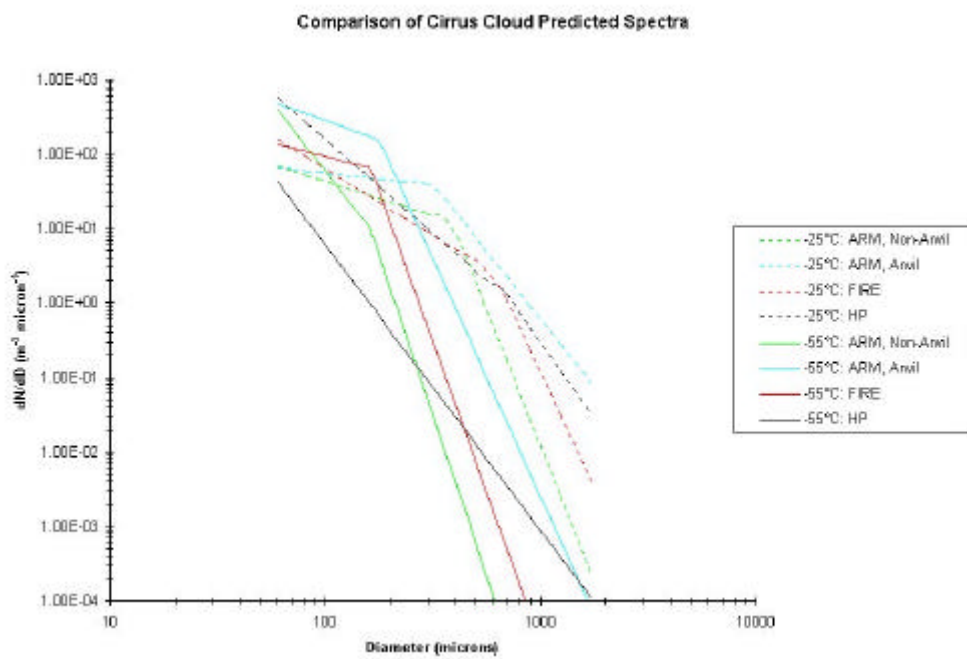| Table 1. Data from ARM 1994.							
Date	**Temperature**	**n**	**Avg. IWC**	N_{100}	**B1**	N_{1000}	**B2**
April	°C		(mg m^{-3})	m$^{-3} \bullet$ m^{-1}		m$^{-3} \bullet$ m^{-1}	
Non- Anvil	> -30	2	35.6122	43.0710	-0.9080	1.211E-02	-7.3179
	< -50	11	3.1259	59.4286	-3.7036	1.532E-06	-8.5976
Anvil	-20 to -30	2	63.1151	55.2670	-0.3132	6.048E-01	-3.6425
	-30 to -40	5	52.5965	95.5644	-0.3994	2.082E-01	-4.9124
	-40 to -50	5	37.2541	252.0676	-1.3000	2.219E-02	-6.1281
	-50 to -60	8	29.0249	280.5713	-1.0562	2.490E-03	-6.3936

Figure 4. Comparison of best-fit size distributions for ARM non-anvil, ARM anvil, FIRE, and HP clouds.
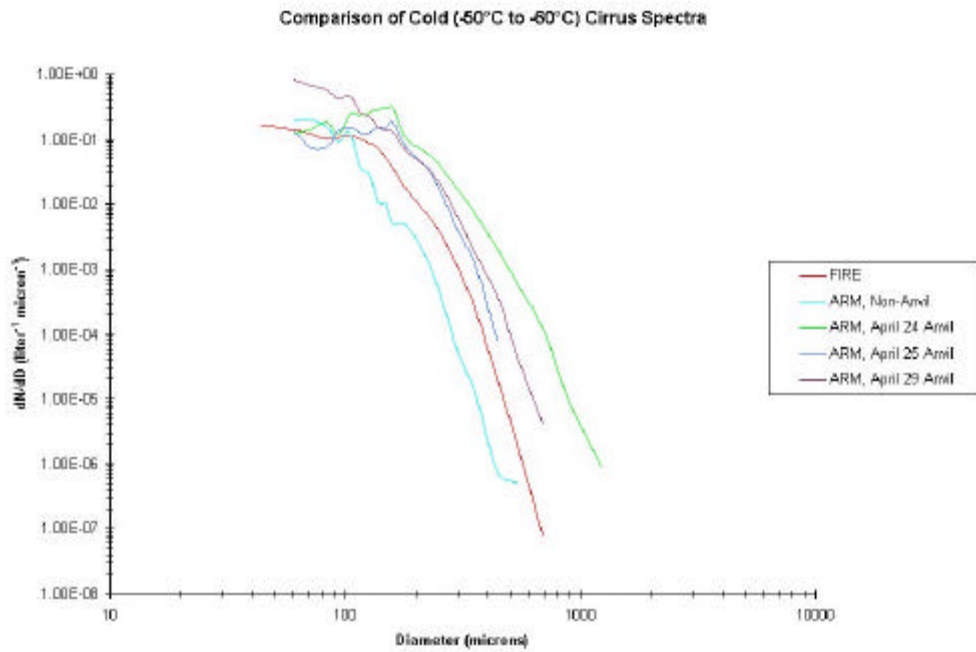
Figure 5. Average size distributions for ARM and FIRE cold cirrus cloud samples.
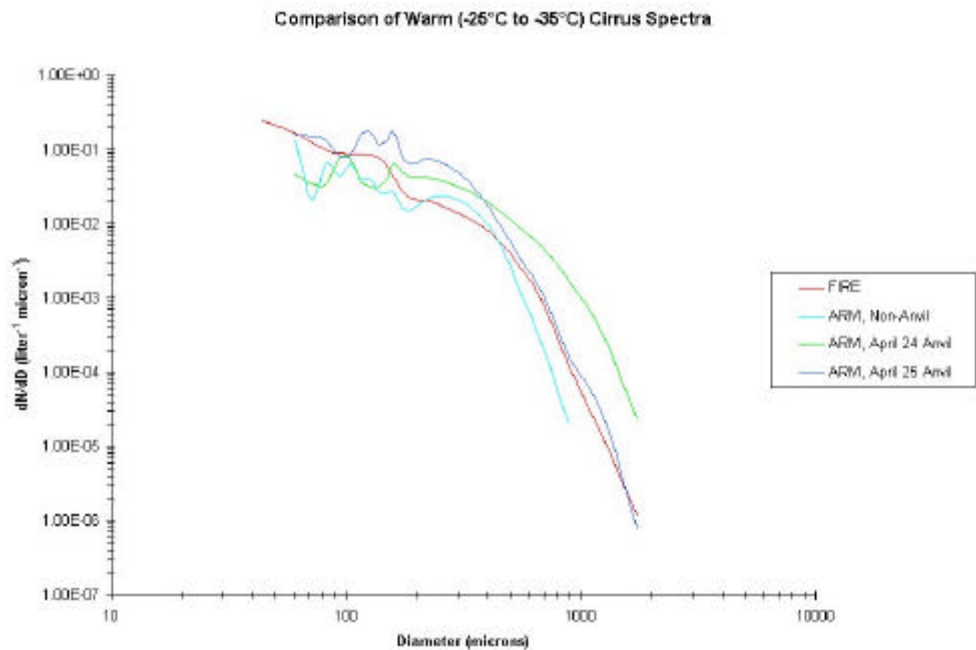

Figure 6. Average size distributions for ARM and FIRE warm cirrus cloud samples.

Finally, the size distributions as a function of position in cloud are shown in Figure 7. A normalized value of 1 represents cloud top. For ARM, only the anvil samples are shown because they comprised approximately 75% of all ARM samples. In general, more large particles were found in the middle and lower portions of the clouds and more small particles were found in the upper cloud regions. This is probably due to aggregation and settling of the larger particles.
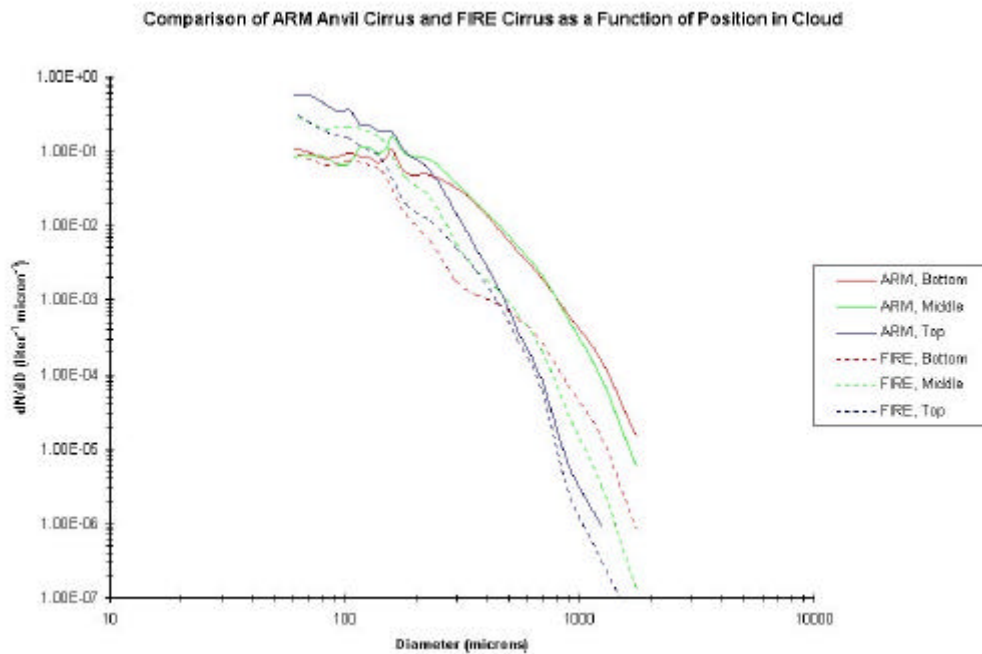

Figure 7. Average size distributions for ARM anvil cirrus and FIRE cirrus as a function of position in cloud.

Ice Water Content

Figure 8 is a scatter plot of IWC as a function of temperature for all 33 ARM samples. IWC was calculated from the replicator data using the technique described in Arnott et al. (1994) and from the 2DC data following Heymsfield (1977). IWC is seen to increase with temperature. Also, the anvil clouds contained more ice mass at a given temperature than the non-anvil clouds except at very cold temperatures.

IWC as a function of position in cloud is shown in Figure 9. For the April 24 and April 25 anvils, the IWC increased sharply from near top to the middle of cloud, which was also found in tropical anvils by McFarquhar and Heymsfield (1996). This is likely the result of sedimentation of the larger particles. The April 29 case, however, shows the reverse trend. This has been attributed to the Eulerian sampling profile used in this IOP. These samples were obtained in a spiral descent over the SGP site. At this time, the anvil structure was patchy and changing rapidly, becoming less dense during the period of descent.
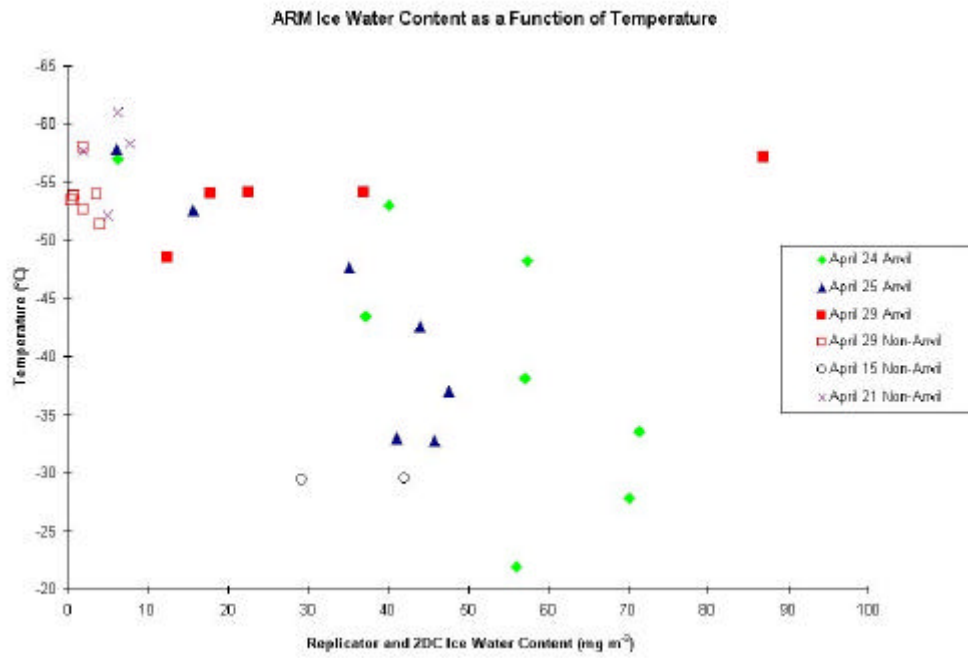
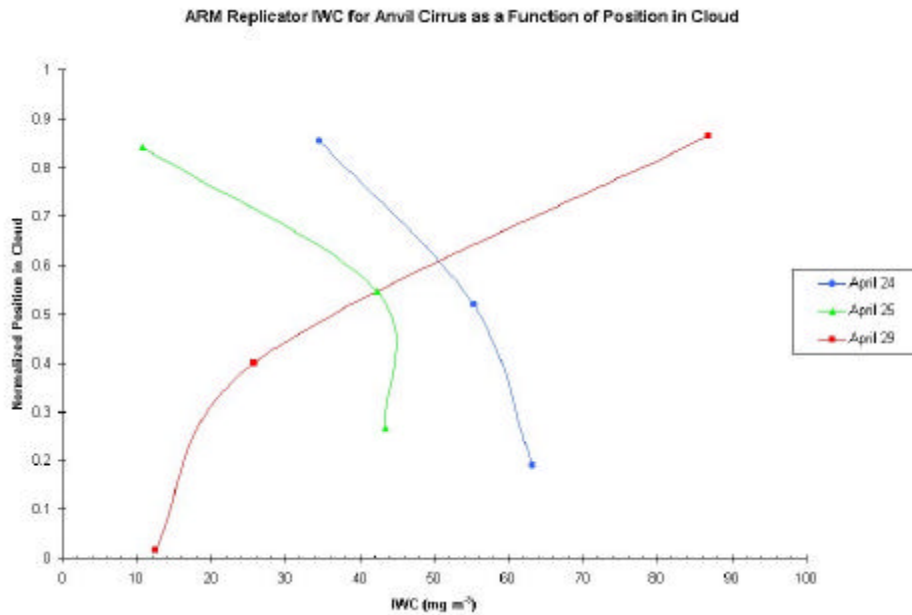**Figure 8**. IWC of ARM cloud samples as a function of temperature.

Figure 9. IWC for ARM anvil cirrus as a function of position in cloud.

Crystal Habit

The crystal habits were determined from the replicator images. Dependence of habit type is shown in Figure 10. Polyplates (as in Figure 11) are seen to be the dominant habit at all temperatures for all flights, with slightly higher percentages at temperatures warmer than -40 °C. The occurrence of columns and polycolumns was greater in the cold cloud samples except near -60 °C. The relative fraction of plates (as in Figure 12) was nearly constant with temperature. These distributions are similar in many respects to those found by HP.

When the habits are considered as a function of position in cloud (Figure 13), the anvil cirrus showed fairly constant percentages overall, with slightly more columnar crystals near cloud top and fewer plates. On the other hand, the non-anvil samples contained a maximum of columns in the lower middle portion of the cloud coinciding with a relative minimum in polyplates. The percentage of plate crystals increased from the lower to the upper cloud regions.
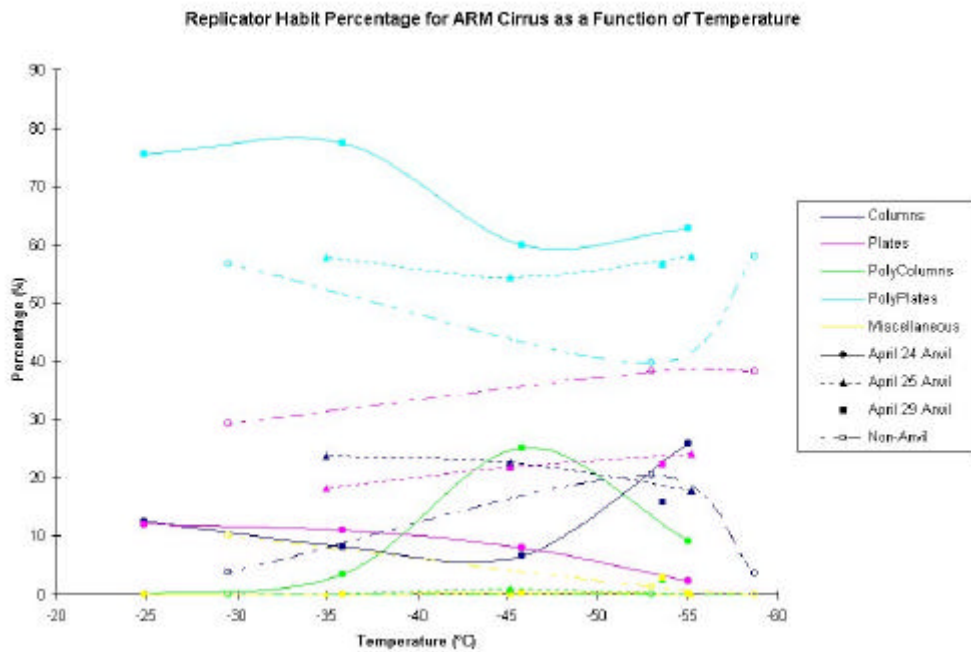

Figure 10. Percentage of crystal habits for ARM cirrus as a function of temperature.
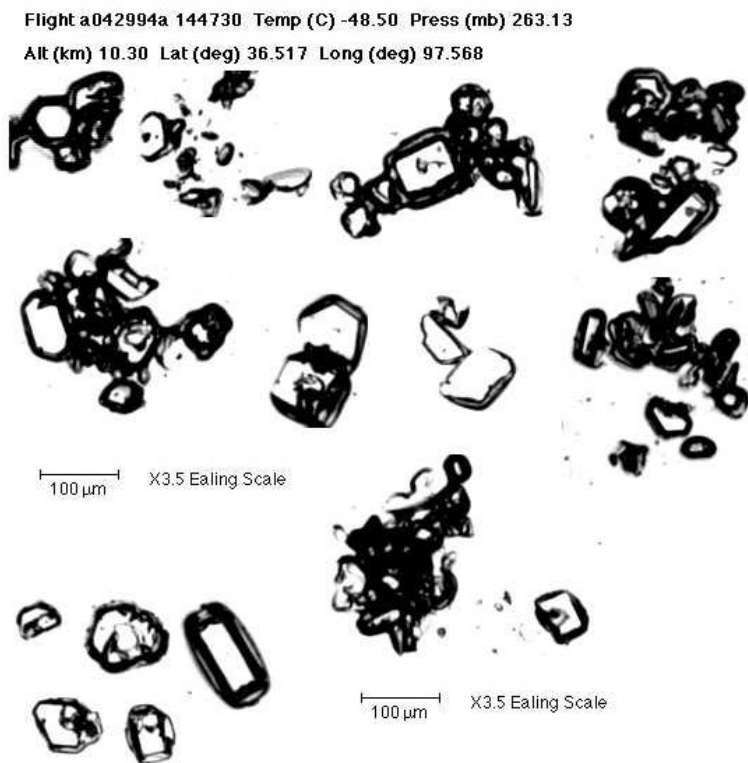
Flight a042994a 144730 Temp (C) -48.50 Press (mb) 263.13
Alt (km) 10.30 Lat (deg) 36.517 Long (deg) 97.568

Figure 11. Replicas of polyplate particles collected on April 29, 1994, at -48.5 °C.

Flight a042994a 145520 Temp (C) -51.49 Press (mb) 251.07
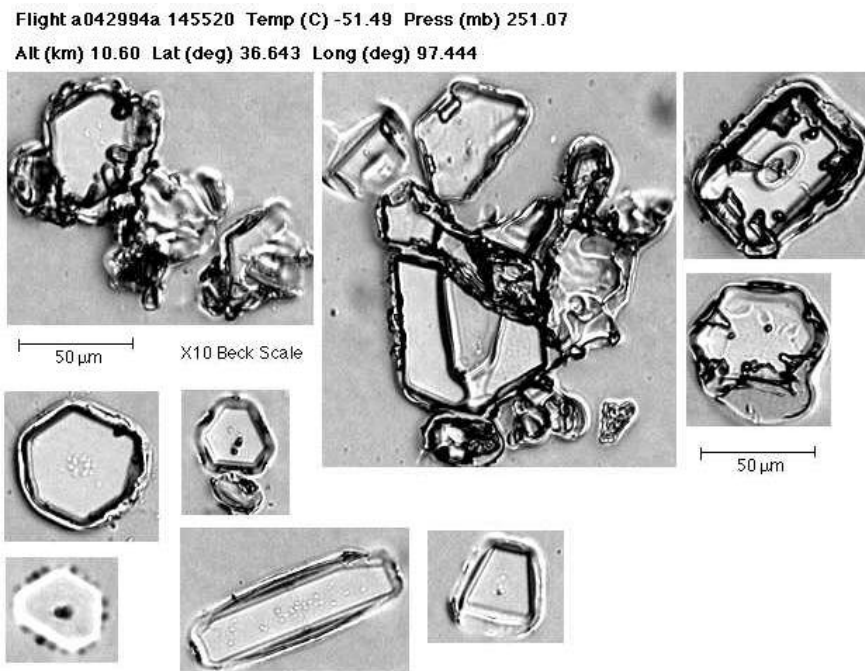Alt (km) 10.60 Lat (deg) 36.643 Long (deg) 97.444

Figure 12. Replicas of plate particles collected on April 29, 1994, at -51.5 °C.
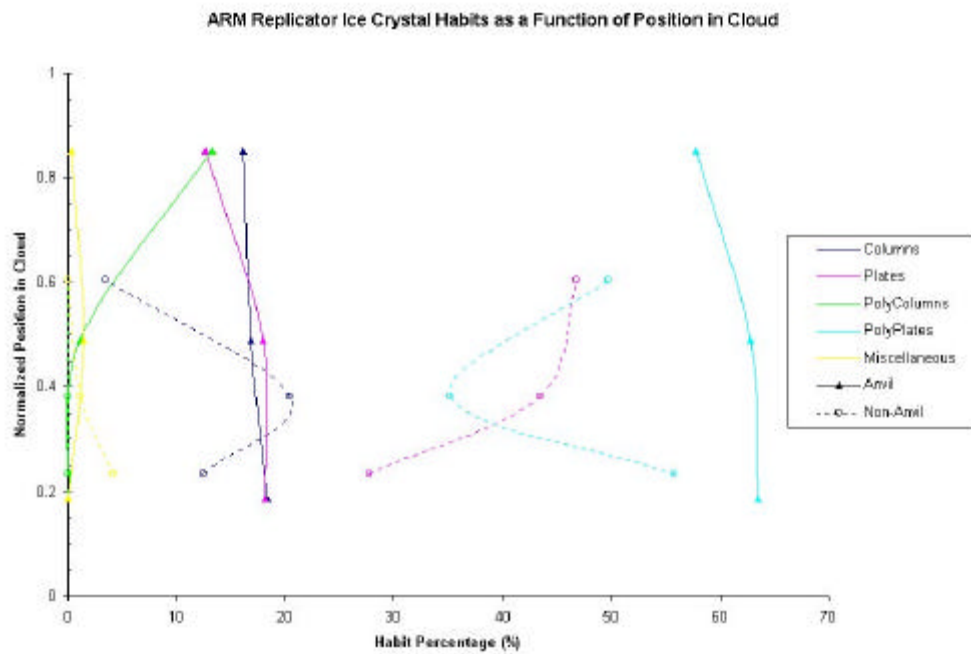
Figure 13. Particle habits as a function of position in cloud.

Conclusions

The data presented here strongly suggest that in order to accurately model the radiative transfer through cirrus, microphysical parameterizations must account for certain differences in cloud properties. Variations in particle size distributions, IWC, and crystal habit are related to factors such as cloud forcing mechanisms and temperature. Model sensitivity to the cloud parameters determined in this study should be tested to determine which of the variations are critical. Because the measured particle sizes did not extend below 50 μm, these results would best be applied to modeling of longwave radiative transfer.

Additional measurements in continental cirrus are needed to better characterize the small end of the particle size distribution and to better understand the variability of the cloud properties. Unfortunately, the sampling strategy employed thus far in taking data over the Cloud and Radiation Testbed (CART) site has been designed almost exclusively to gather in situ data for comparison with ground-based observations. Flight profiles have been of either Eulerian spiral or short step climb/descent form. A better understanding of the clouds would be achieved through Lagrangian spirals and long-leg step patterns. This should be considered for future cloud IOP operations.

References

Arnott, W. P., Y. Y. Dong, J. Hallett, and M. R. Poellot, 1994: Role of small ice crystals in radiative properties of cirrus: A case study, FIRE II, November 22, 1991. *J. Geophys. Res.*, **99**, 1371-1381.

Heymsfield, A. J., 1977: Precipitation development in stratiform ice clouds: A microphysical and dynamical study. *J. Atmos. Sci.,* **34**, 367-381.

Heymsfield, A. J., and C. M. R. Platt, 1984: A parameterization of the particle size spectrum of ice clouds in terms of the ambient temperature and the ice water content. *J. Atmos. Sci*., **41**, 846-855.

McFarquhar, G. M., and A. J. Heymsfield, 1996: Microphysical characteristics of three anvils sampled during the Central Equatorial Pacific Experiment. *J. Atmos. Sci.,* **53**, 2401-2423.

Poellot, M. R., R. Zerr, W. P. Arnott, and J. Hallett, 1998: A microphysical characterization of cirrus from the FIRE-II Cirrus IFO. Preprints, Conference of Cloud Physics, Everett, Washington, 3-6.